Radar Imaging: Side Looking Radar (SLR)

In remote sensing, the view is to the side and the motion of the airplane or spacecraft allows an image to be built up, line by line.

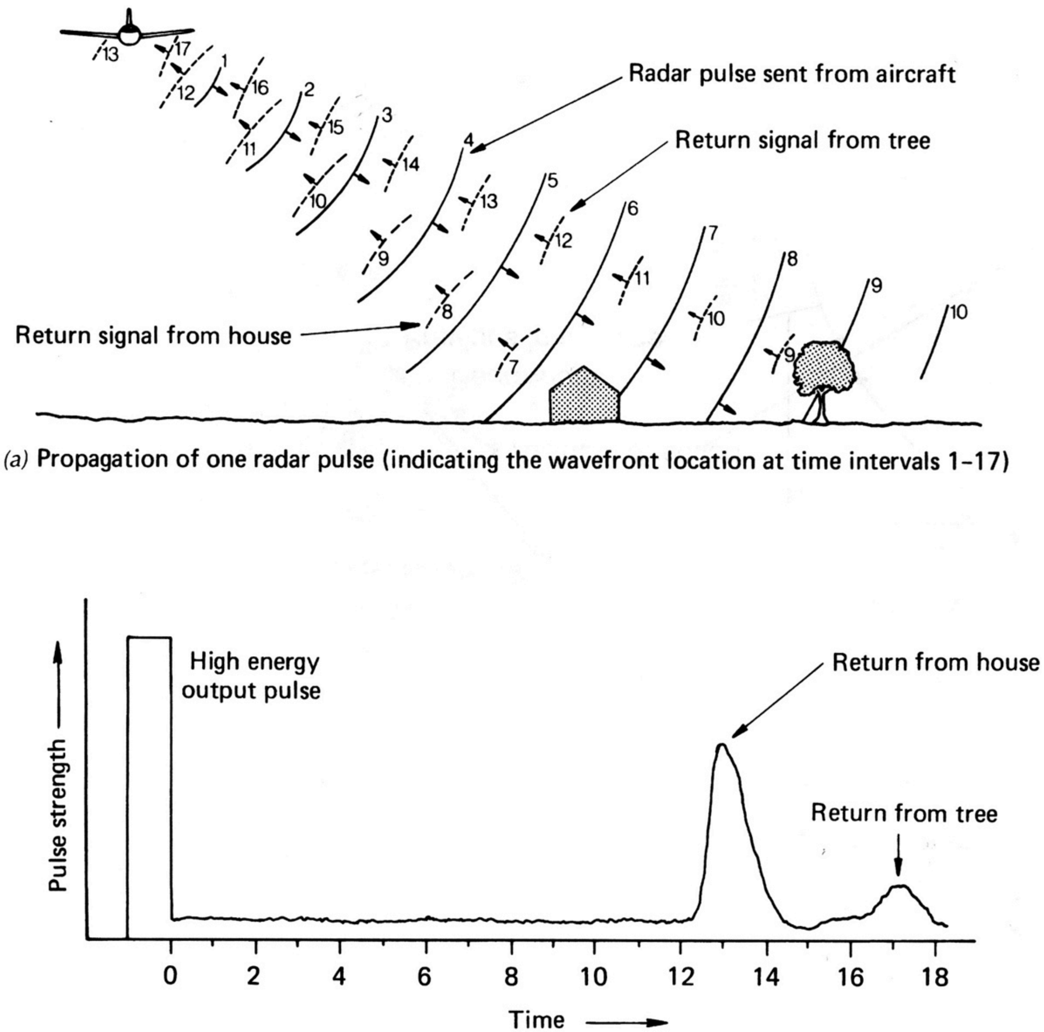

(a) Propagation of one radar pulse (indicating the wavefront location at time intervals 1–17)

(b) Resulting antenna return

Figure 8.1 Operating principle of SLR.

Geometric Terms in Side-Looking Radar

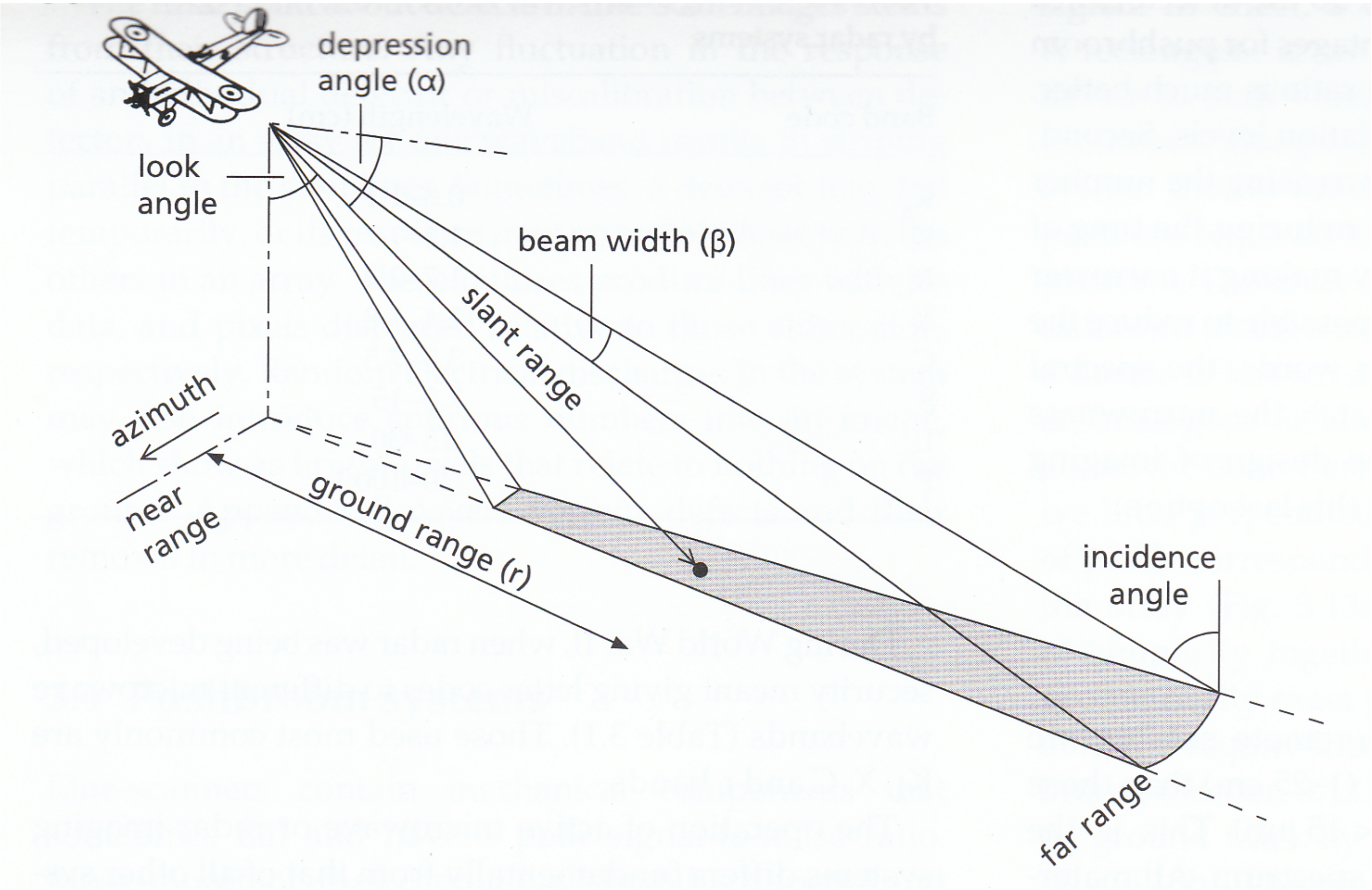

SLR Spatial Resolutions

Range Resolution (perpendicular to flight track):

$$R_r = \frac{\tau c}{2\cos\gamma}$$

τ in μs, c=3x10^8 m/s

Azimuth Resolution (along flight track):

$$R_a = \frac{0.7 \cdot S \cdot \lambda}{D}$$

R_a in cm, S in km, λ and D in cm.

Two features are resolved in the range direction if their return pulses do not arrive back at the antenna at the same time.

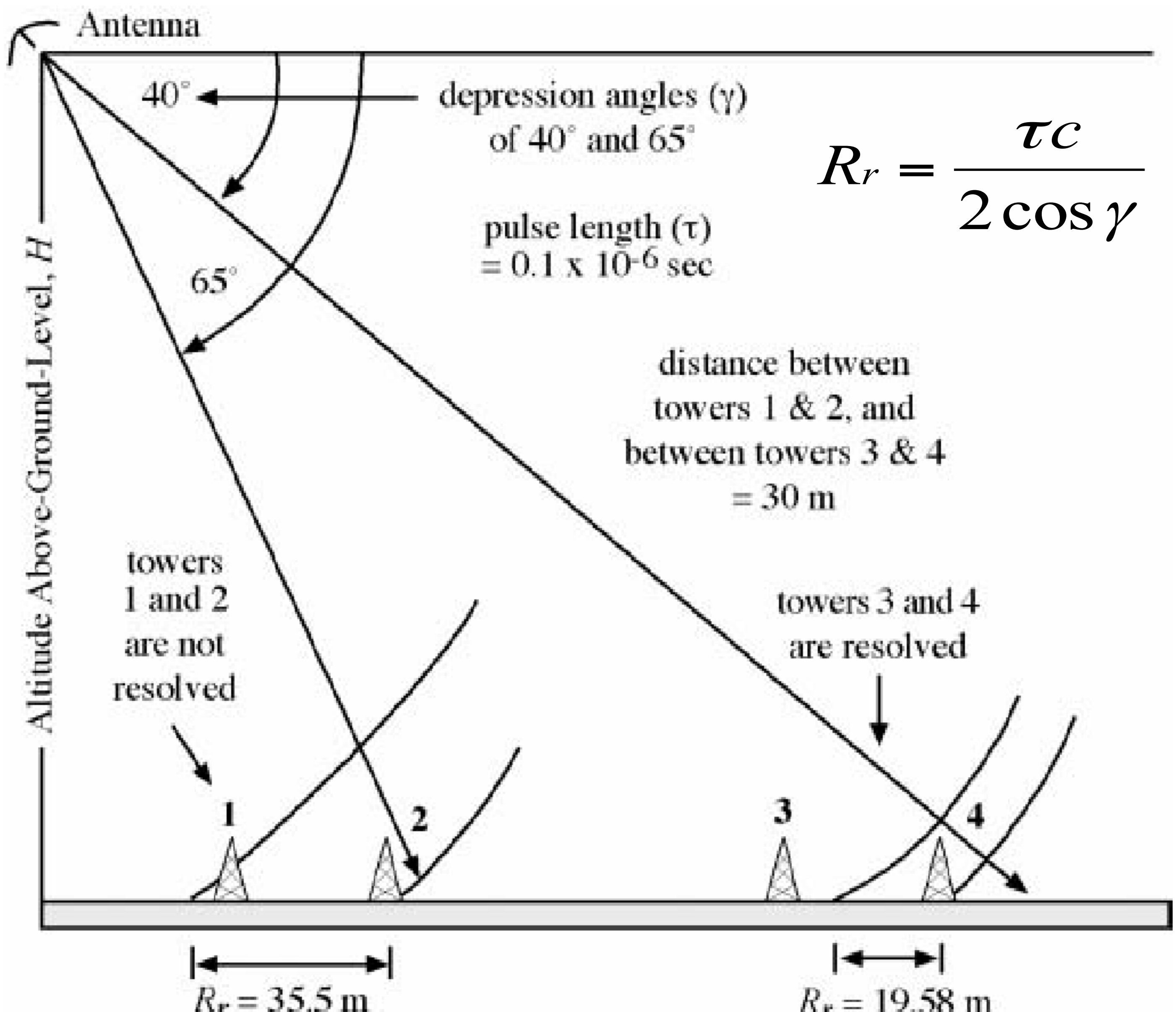

$$R_r = \frac{\tau c}{2 \cos \gamma}$$

Range Resolution

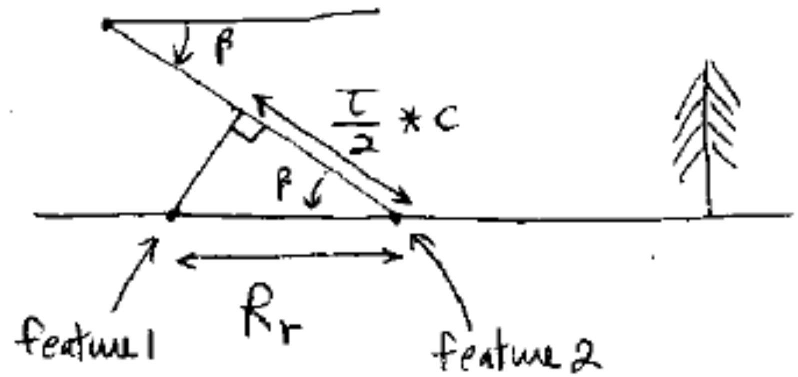

- Pulse length in distance is $\tau * c$.
- Assume that features are separated in range direction if range separation is greater than $(\tau * c)/2$.
- From the triangle in diagram, we can derive equivalent horizontal resolution (R_r).
- As pulse length and depression angle decrease, the resolution gets smaller. Better resolution further from the antenna.
- As depression angle increases for points closer to the antenna, resolution is worse.
- Another reason why radar can not image directly beneath the antenna.

$$\cos\beta = \frac{\frac{\tau}{2} \times c}{R_r}$$

And

$$R_r = \frac{\tau \times c}{2\cos\beta}$$

$$R_a = \frac{0.7 \cdot S \cdot \lambda}{D}$$

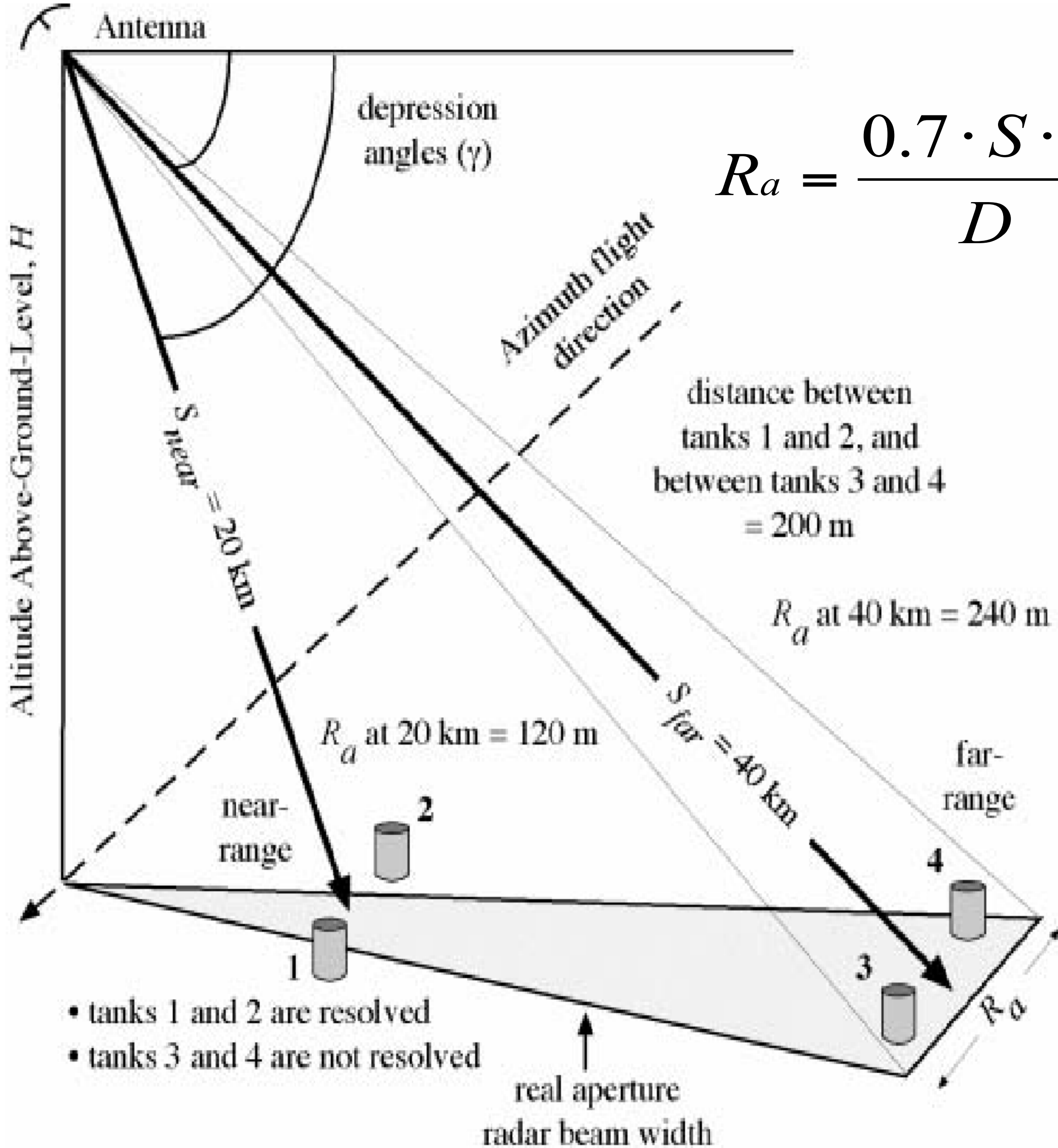

Along-track resolution is better ***closer*** to the antenna

SAR Azimuth Resolution

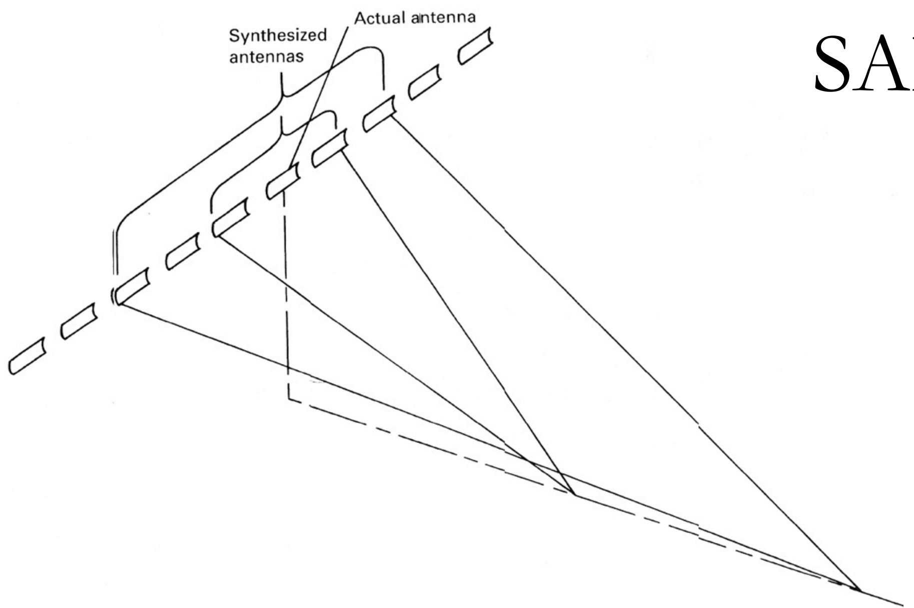

Figure 8.8 Coончcept of an array of real antenna positions forming a synthetic aperture.

Azimuth resolution in a simple radar is defined by the beam width. But modern radars are *synthetic aperture radars*, which use the Doppler shift of the returned signal to narrow the azimuthal resolution of the instrument.

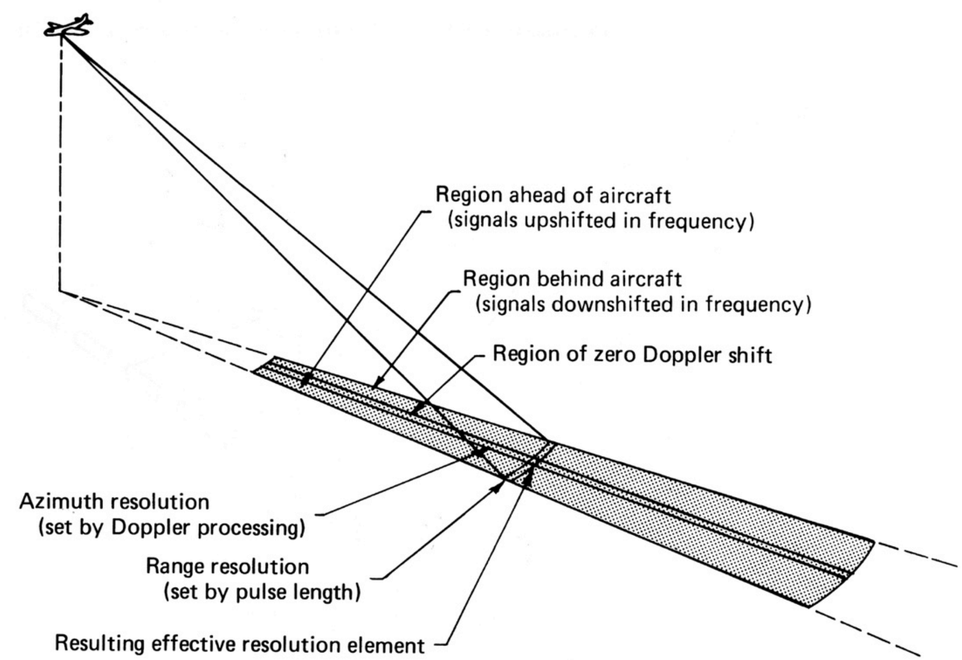

Figure 8.9 Determinants of resolution in synthetic aperture SLR.

Radar interactions with the surface

Surface properties affecting returned signal:

- Feature orientation and slopes
- Dielectric properties of surface material

  Dry rock and soil: 3 to 8 (good absorbers)

  Water: 80 (good reflector)

  Mostly affects penetration depth. 1% water blocks penetration.

- Characteristic surface roughness scale

Dielectric Constant

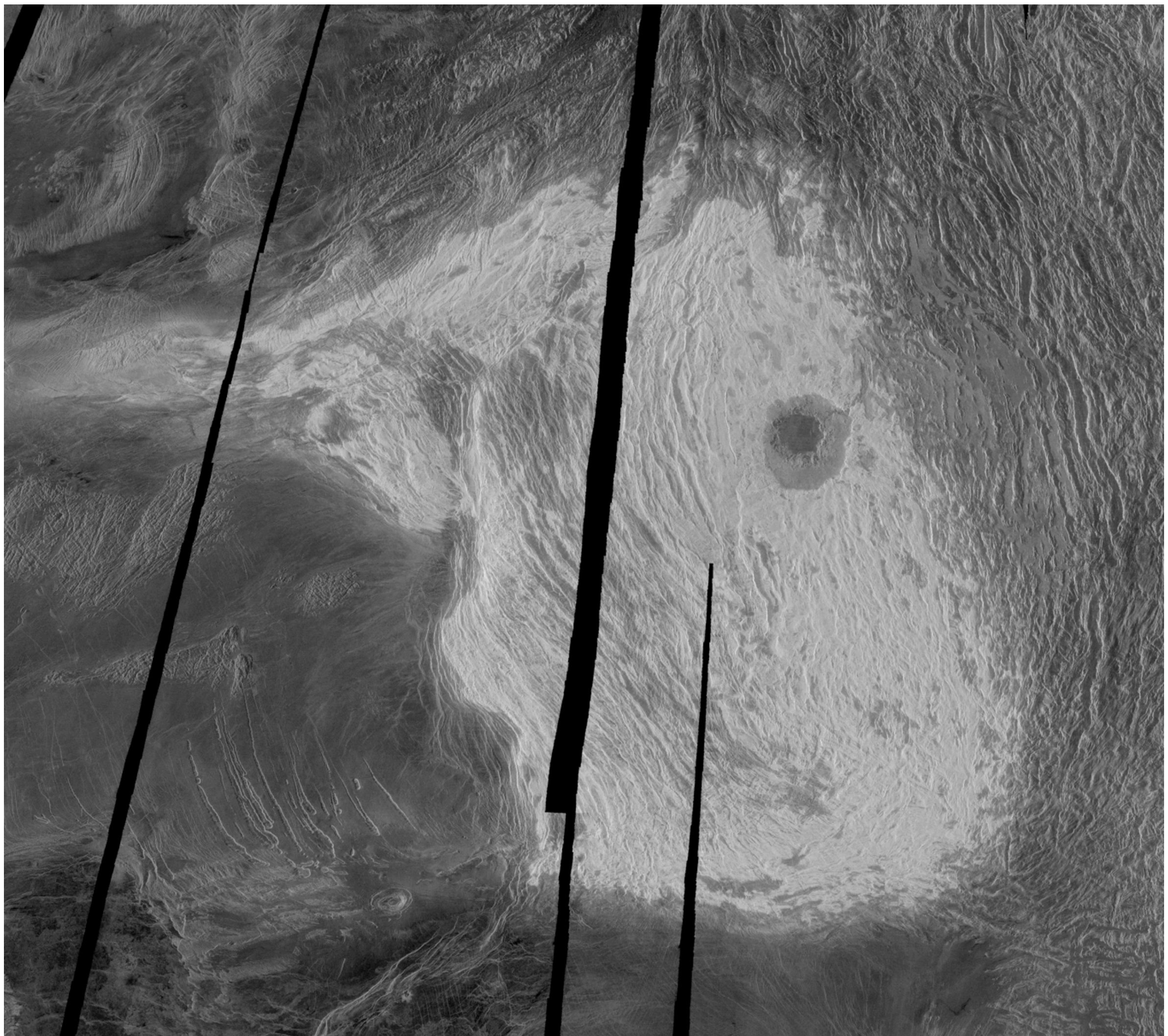

Maxwell Montes, Venus
(pyrite?)

Effect of Wavelength

Two main factors:

(1) Response to roughness

(2) Penetration of vegetation canopy and ground

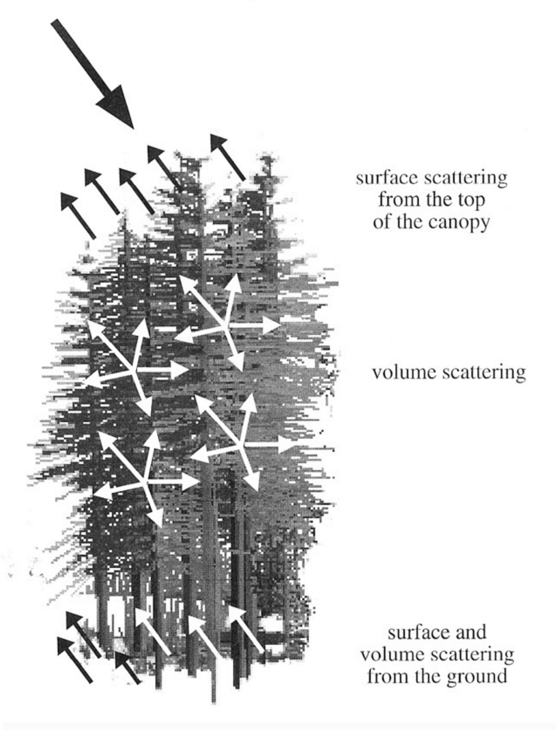

Figure 9-22 The types of active microwave surface and volume scattering that might take place in a hypothetical pine forest stand (after Carver, 1988).

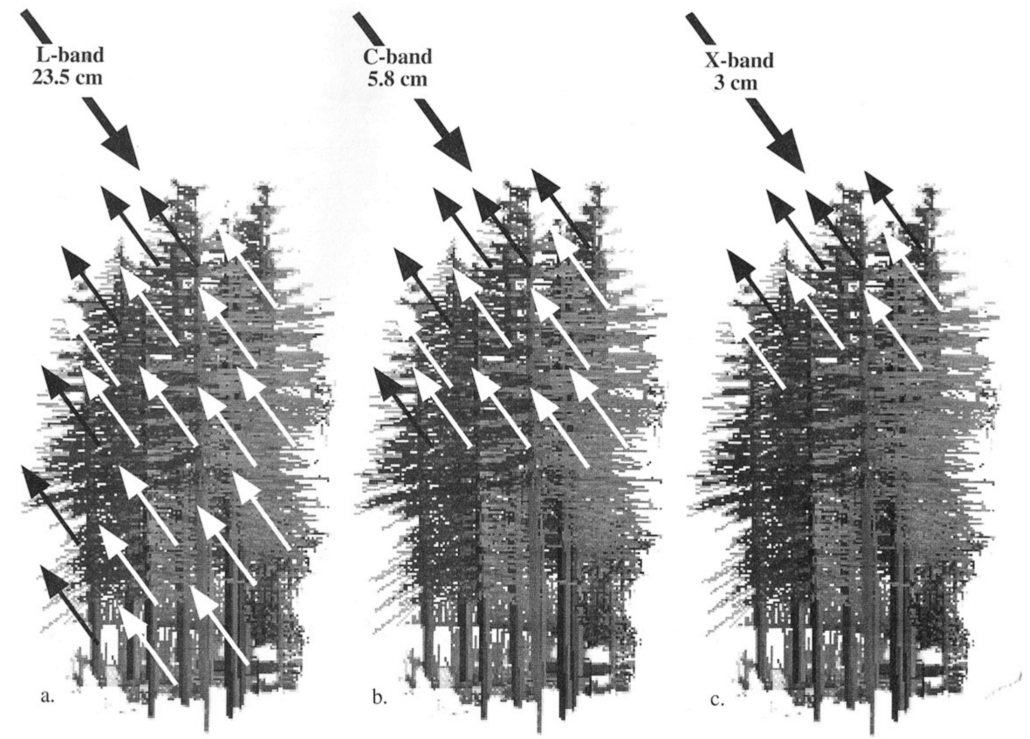

Figure 9-23 Theoretical response of a pine forest stand to X-, C-, and L-band microwave energy. The shorter the wavelength, the greater the contribution from *surface scattering*. The longer the wavelength, the greater the penetration into the material and the greater the *volume scattering*.

Types of Scattering

- Surface scattering from relatively smooth surfaces will be specular (Fresnel) or quasi-specular.
- Scattering from a surface rough at the scale of the wavelength will be diffuse.
- If the material is relatively lossless, then volume penetration and subsurface scattering or quasi-specular reflection from layers may occur.

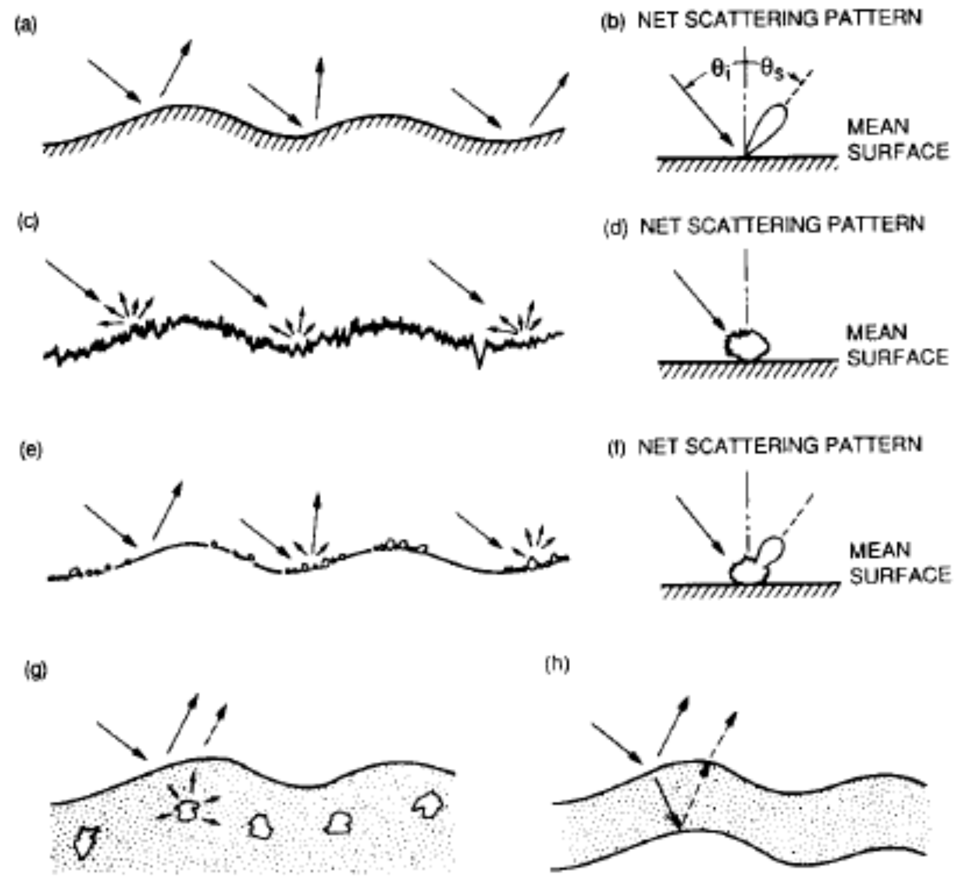

Radar Imaging: Side Looking Radar (SLR)

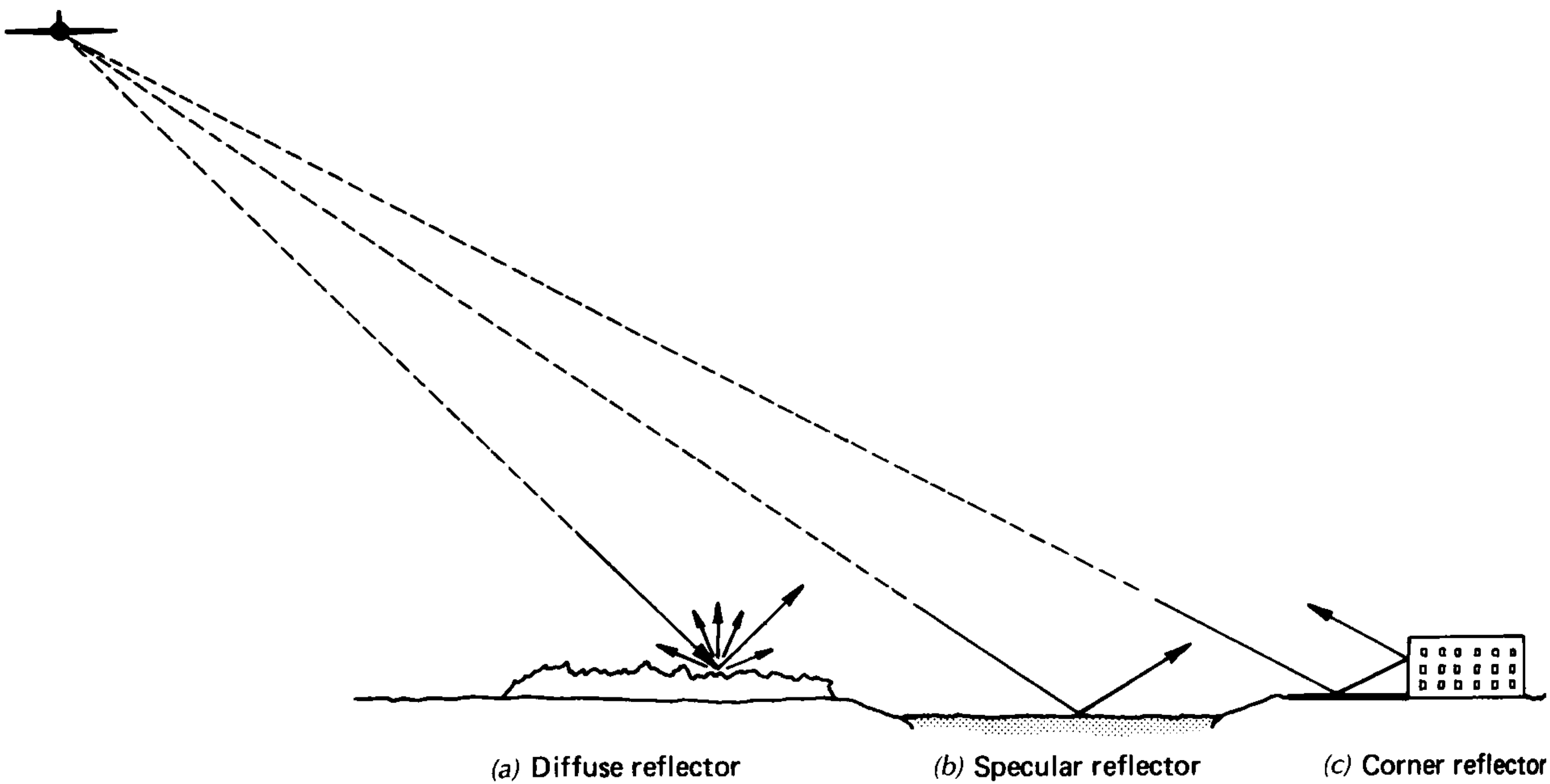

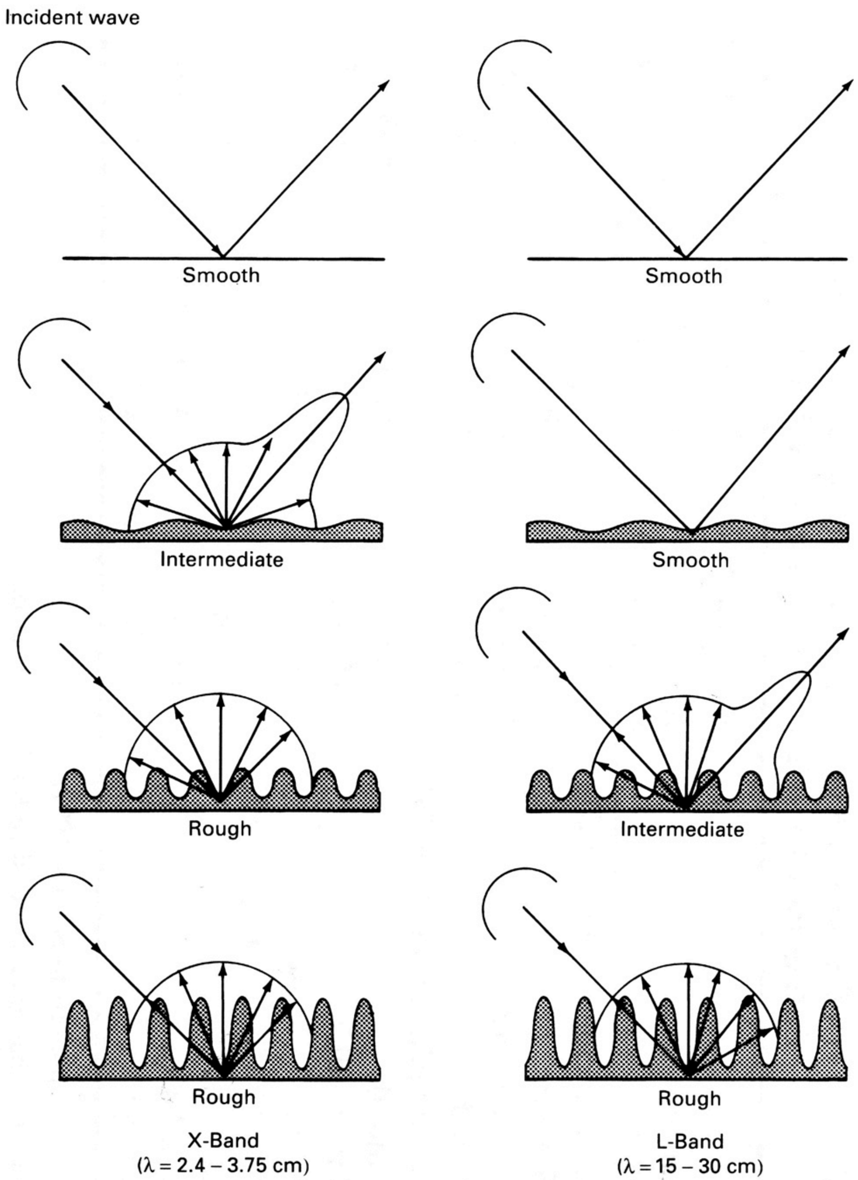

Figure 8.23 X-band and L-band radar reflection from surfaces of varying roughness. (Modified from diagram by Environmental Research Institute of Michigan.)

Surface Roughness and Backscatter

"Rough" is defined with respect to the wavelength of the radar.

TABLE 8.3 Synthetic Aperture Radar Roughness at a Local Incident Angle of 45°

Root-Mean-Square Surface Height Variation (cm)	K_a Band (λ = 0.86 cm)	X Band (λ = 3.2 cm)	L Band (λ = 23.5 cm)
0.05	Smooth	Smooth	Smooth
0.10	Intermediate	Smooth	Smooth
0.5	Rough	Intermediate	Smooth
1.5	Rough	Rough	Intermediate
10.0	Rough	Rough	Rough

Source: Adapted from Sabins, 1997.

Rayleigh Criterion

$$h = \frac{\lambda}{8\cos I}$$

<3 cm – smooth
>3 cm - rough

(for L band)

h = rms height
I = incidence angle

<u>3-stage classification</u>

Smooth: < 1cm
Intermediate: 1 – 5 cm
Rough: > 5 cm

$$h = \frac{\lambda}{25\cos I}$$

$$h = \frac{\lambda}{4.4\cos I}$$

Effect of Surface Roughness as a Function of Incidence Angle

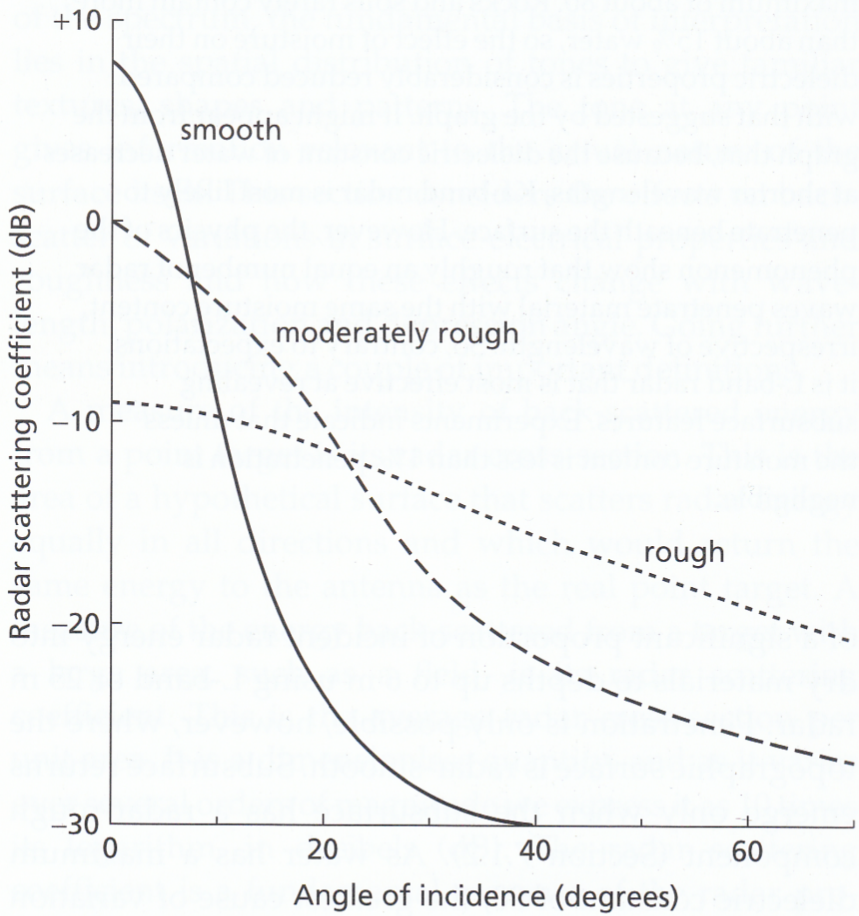

Fig. 7.3 The proportion of emitted energy back-scattered from a surface to the antenna—the radar scattering coefficient—depends on both the surface roughness and the angle of incidence. Both the depression angle and the surface slope control the incidence angle.

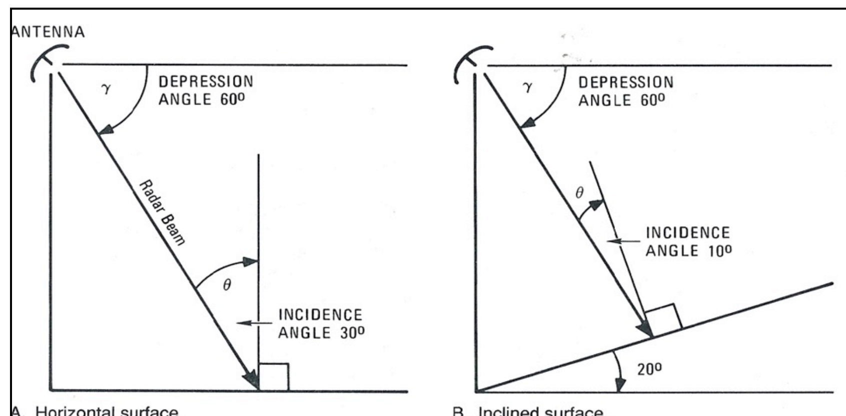

Figure 6-5 Depression angle and incidence angle.

Geometric Factors: Topographic Relief

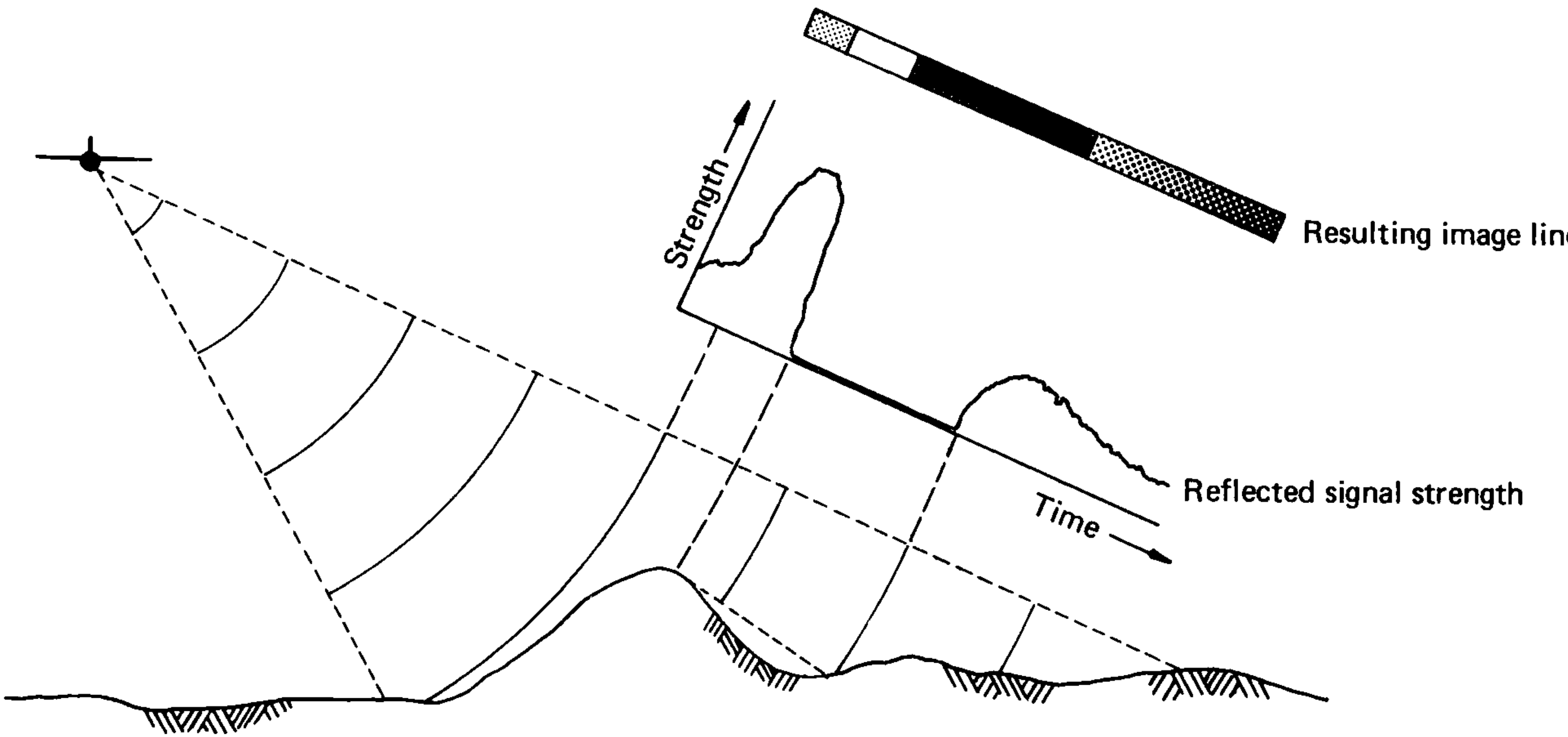

Geometric Factors: Orientation

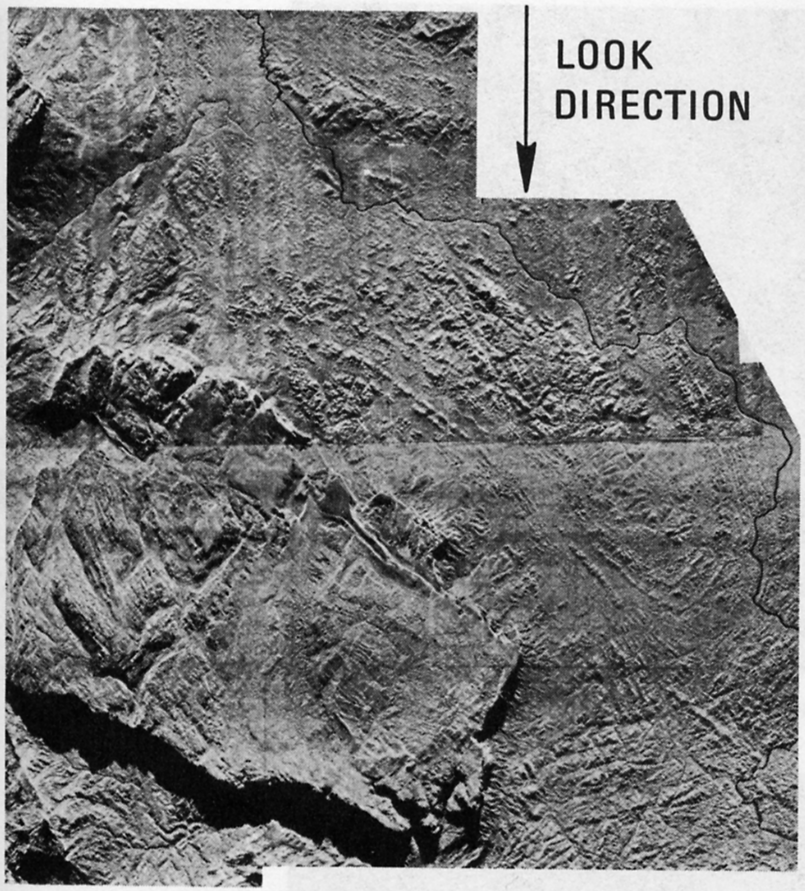

A. Look direction toward south.

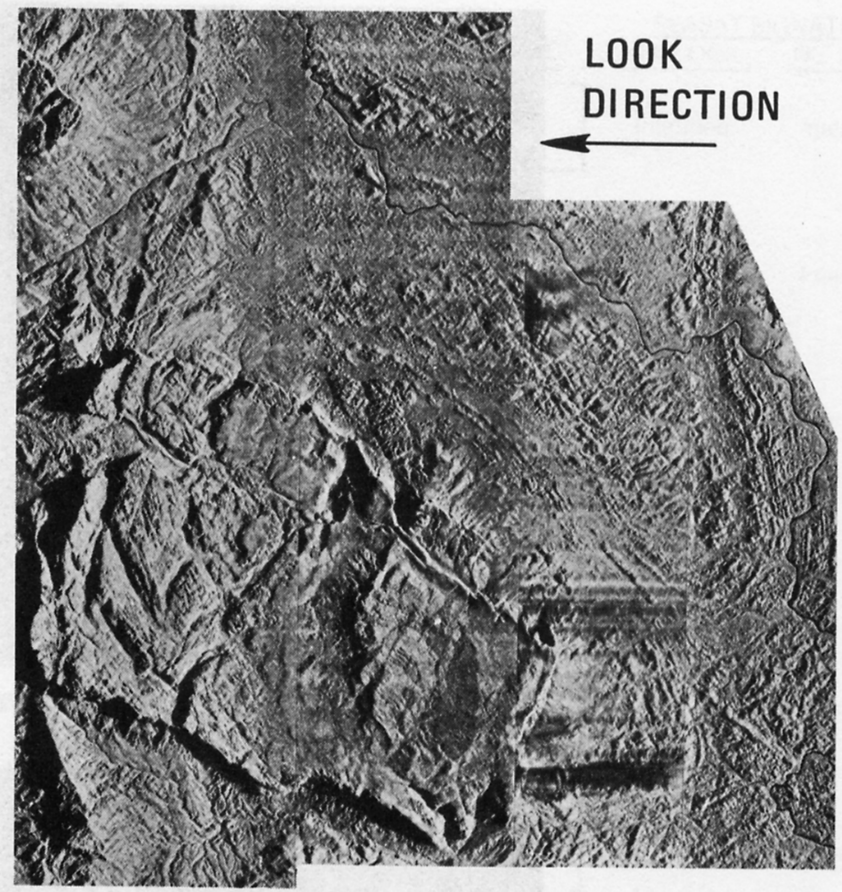

B. Look direction toward west.

Radar Shadows

- Radar shadows occur when slopes are not seen by radar beam. That is, when slope angle is greater than the depression angle.
- Shadow lengths get longer behind obstacles as depression angle gets smaller.

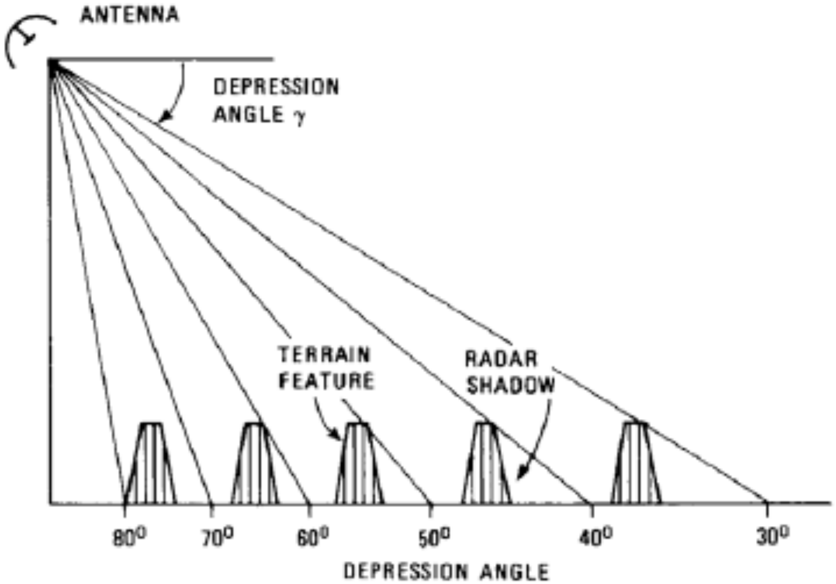

A. Cross-section view.

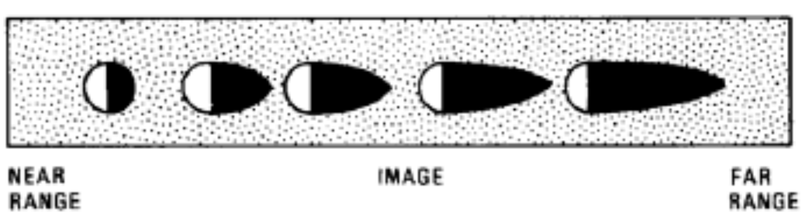

B. Map view.

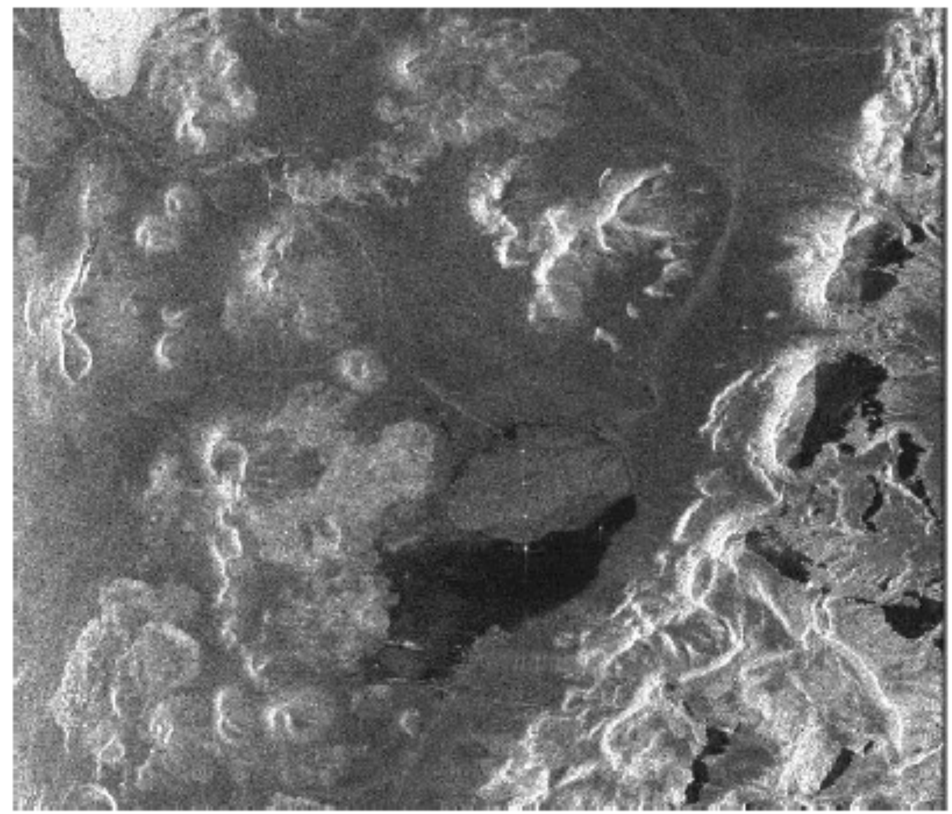

A. Radar image.

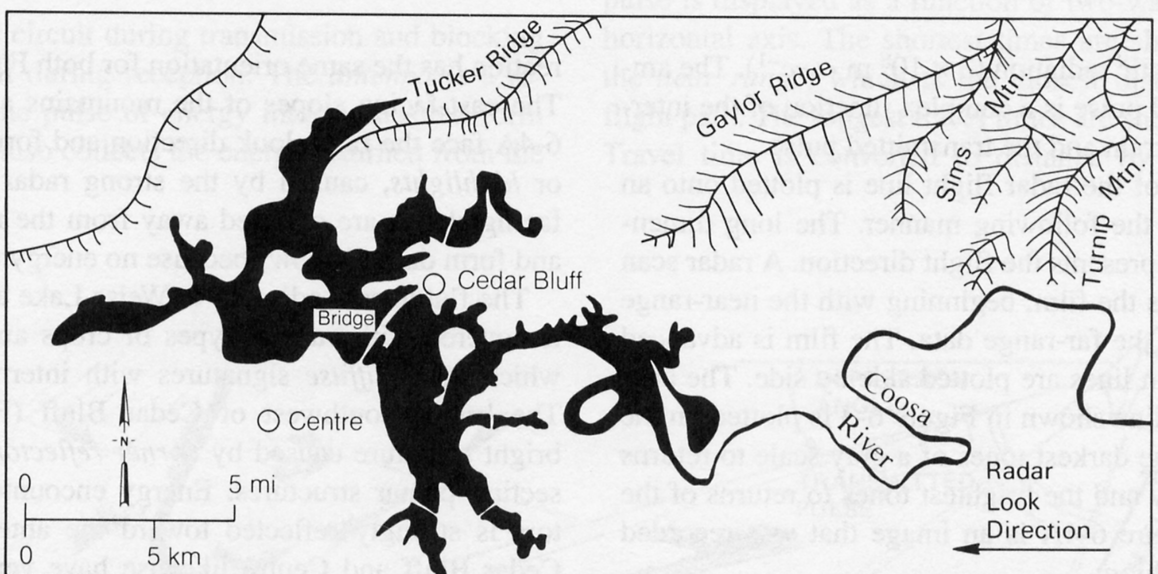

B. Location map.

Dihedral and Trihedral Reflectors

- Reflected rays from dihedral reflector appear to come from intersection of horizontal and vertical surfaces because path length (and thus travel time) is the same for all paths.
- Reflected rays from trihedral reflectors (e.g., corner reflector) appear to come from single point at center of the corner for same reason.

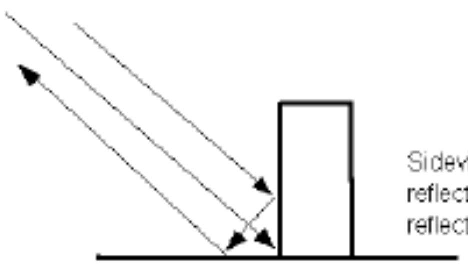

Sideview of a dihedral reflector with Fresnel reflection dominating

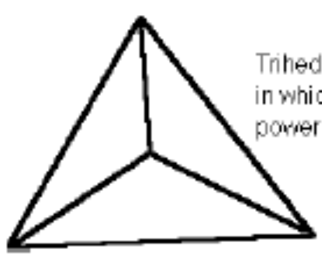

Trihedral or corner reflector in which all Fresnel reflected power appears to come from center

- Corner reflectors are used for radar image calibration.

Corner Reflectors

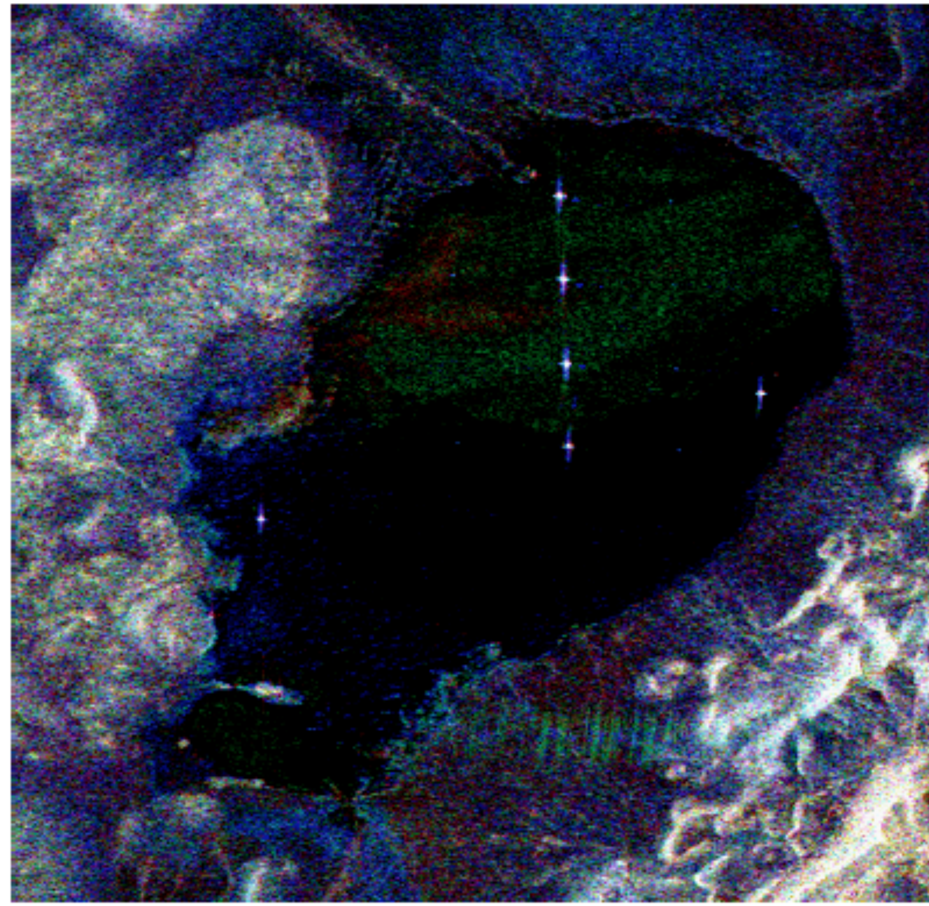

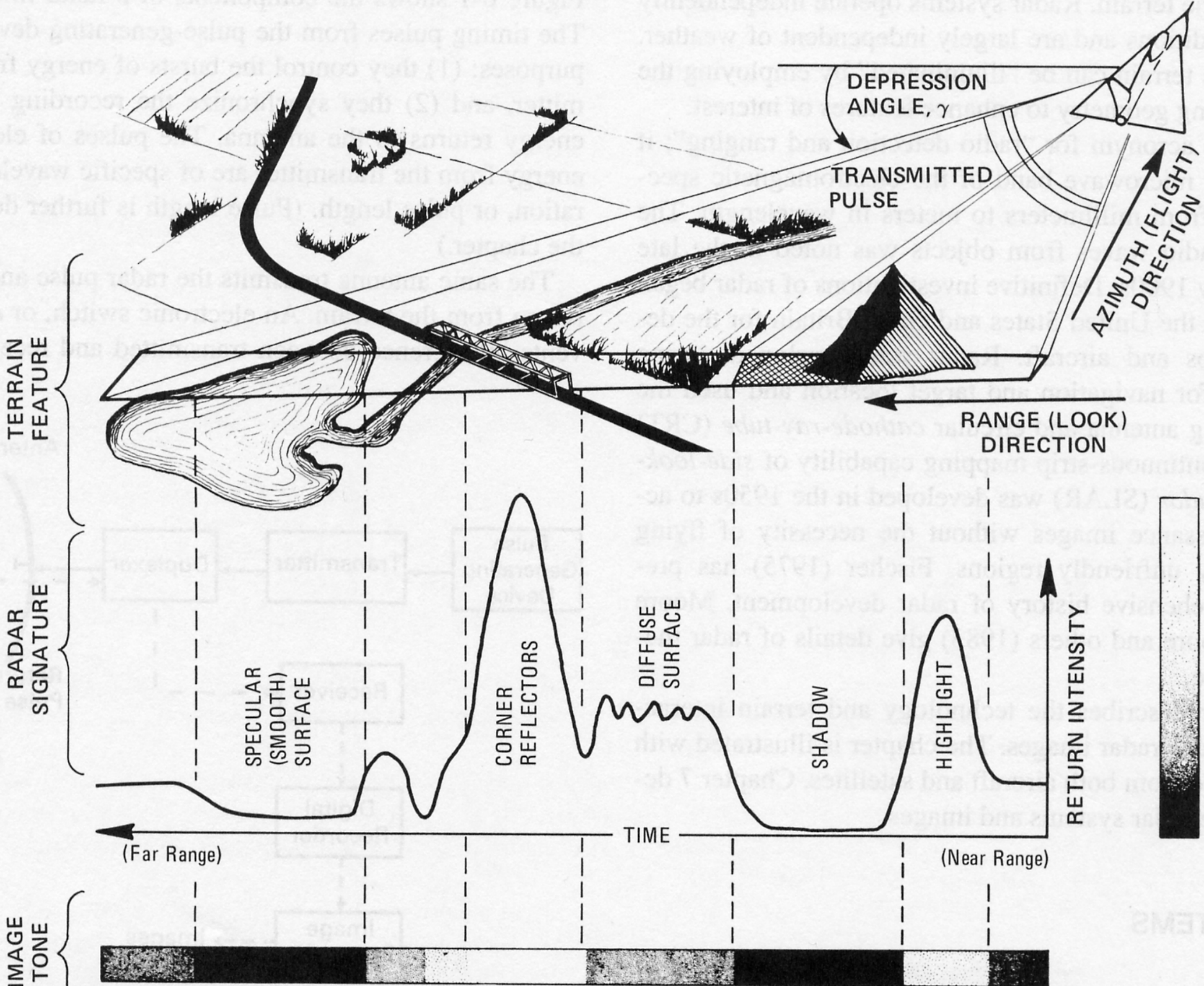

Figure 6-3 Terrain returns and image signatures for a pulse of radar energy.

Foreshortening

- Given that range determines cross-track pixel location, there is geometric foreshortening.
- Cross-track length of feature determines how long it remains in radar illumination.
- If surface slope is normal to wave front, then slope appears as a point in output image.
- Foreshortening is one reason why radar is side-looking. Features directly beneath aircraft would have same return times and thus show as single point.

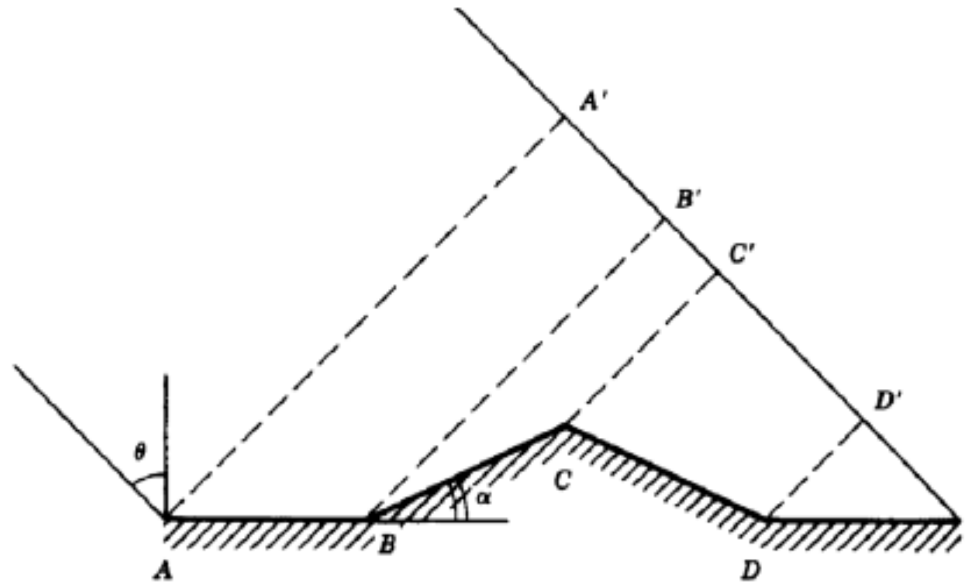

$$A'B' = AB \sin\theta$$
$$B'C' = BC \sin(\theta - \alpha)$$
$$C'D' = CD \sin(\theta + \alpha)$$

Foreshortening

- Surfaces seen with largest depression angles (closest to antenna) will have greatest amount of foreshortening.
- Foreshortening decreases as the depression angle decreases (i.e., further from antenna) for a given surface slope.
- Example of foreshortening for slopes of 15º from horizontal.

Depression Angle	Foreshortening (fore slope)	Foreshortening (back slope)
75	0.0 (point)	0.50
55	0.34	0.77
45	0.50	0.87
25	0.77	0.98
15	0.87	1.00 (true length)

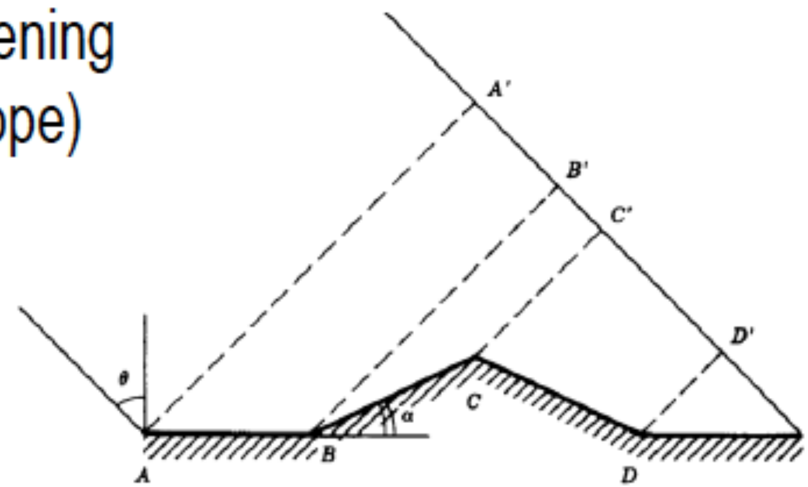

$$A'B' = AB \sin\theta$$
$$B'C' = BC \sin(\theta - \alpha)$$
$$C'D' = CD \sin(\theta + \alpha)$$

Foreshortening Example

- Seasat image of Alaska. Radar illumination is from the top.

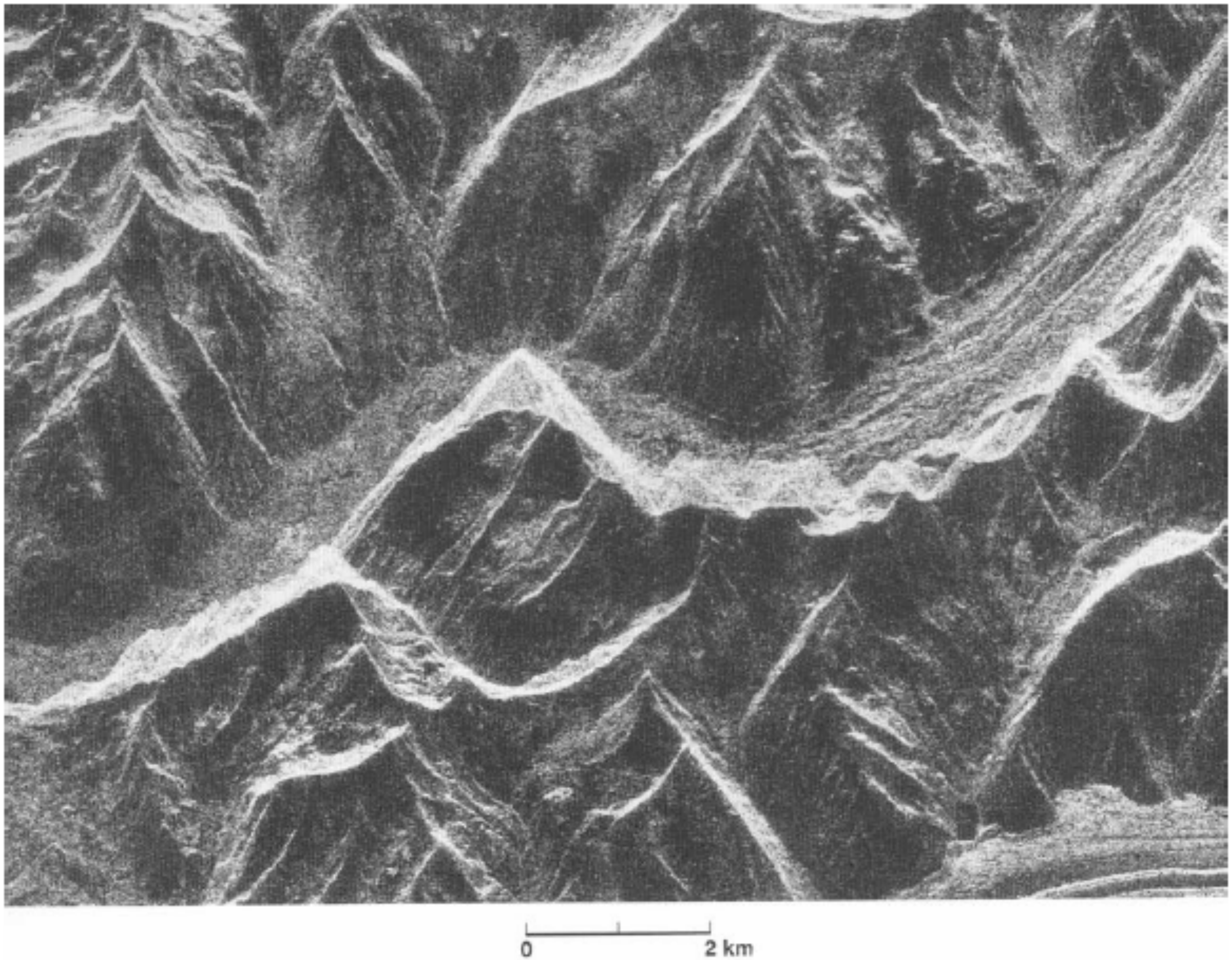

Layover in Radar Images

- Layover occurs when slopes are so steep that return from top of slope is received before the return from the bottom of slope.
- Object appears to be "laying over" on its side in the radar image.
- Layover increases as depression angle increases.

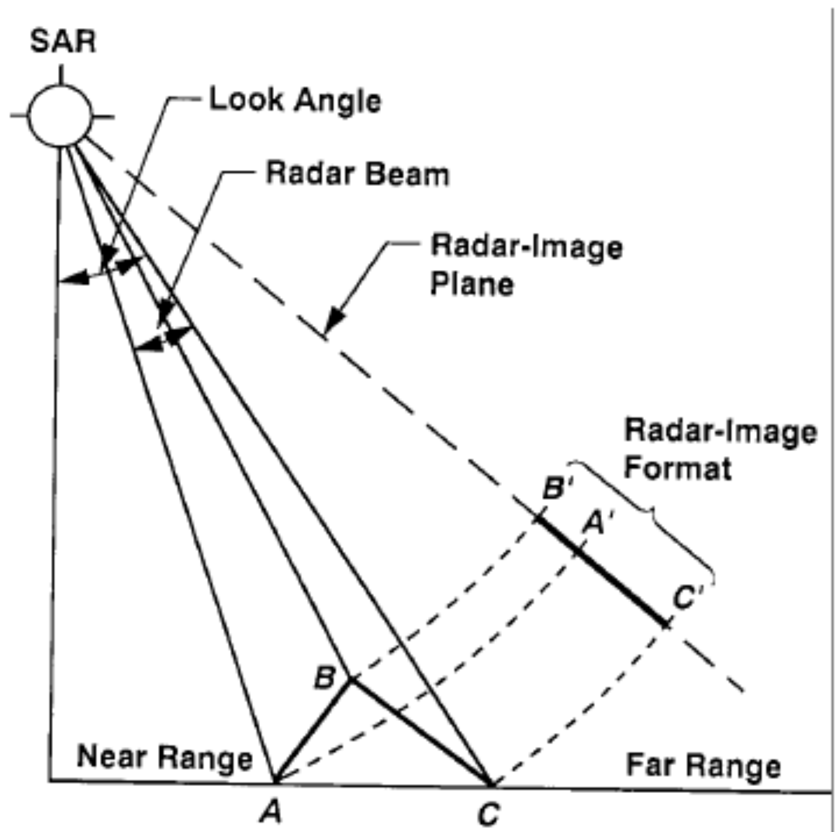

Layover

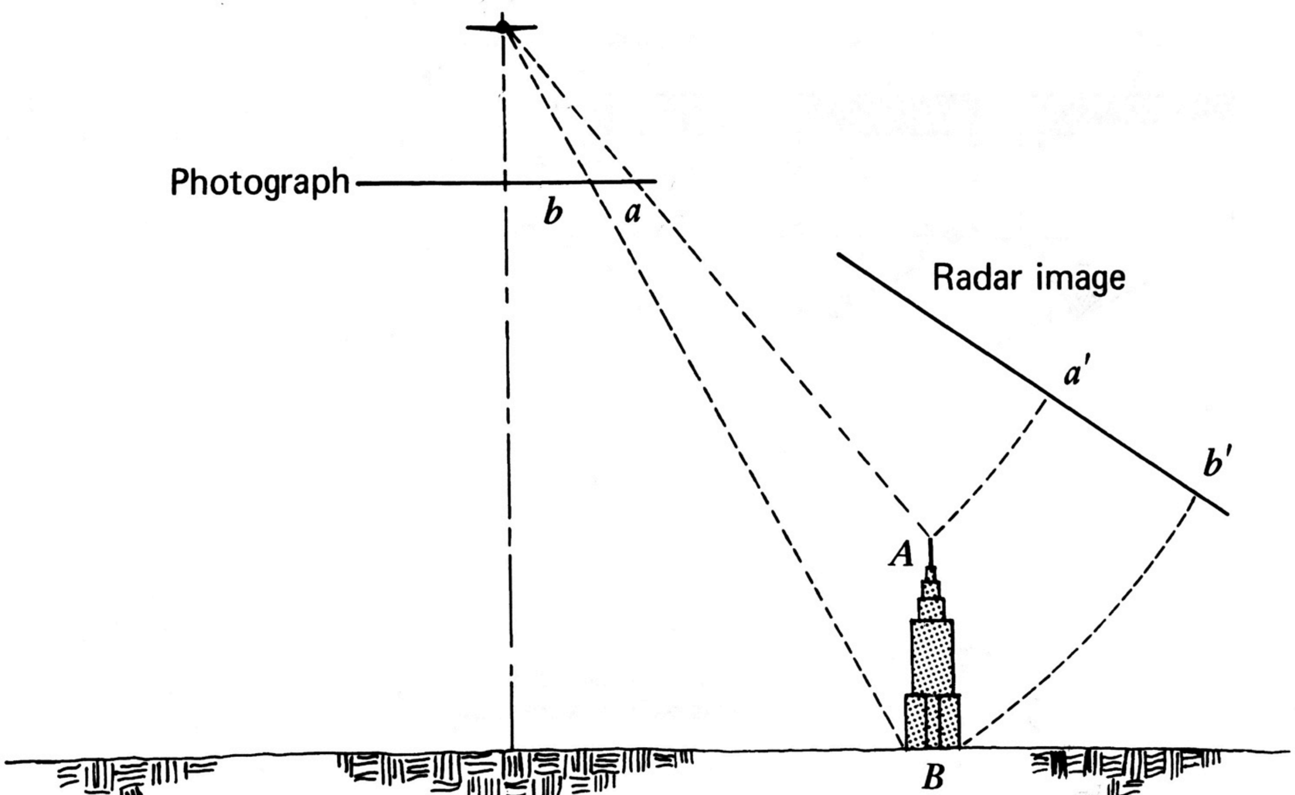

Figure 8.12 Relief displacement on SLR images versus photographs.

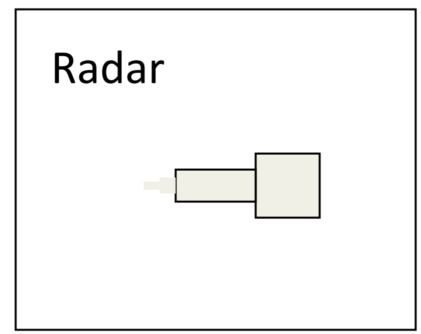

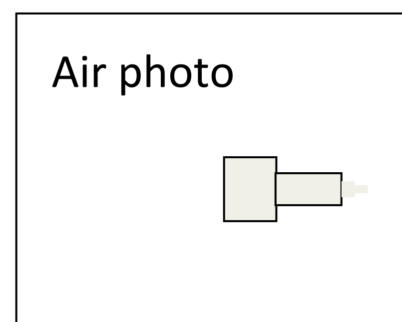

Layover Example

- Seasat image of Alaska. Radar illumination is from the top.

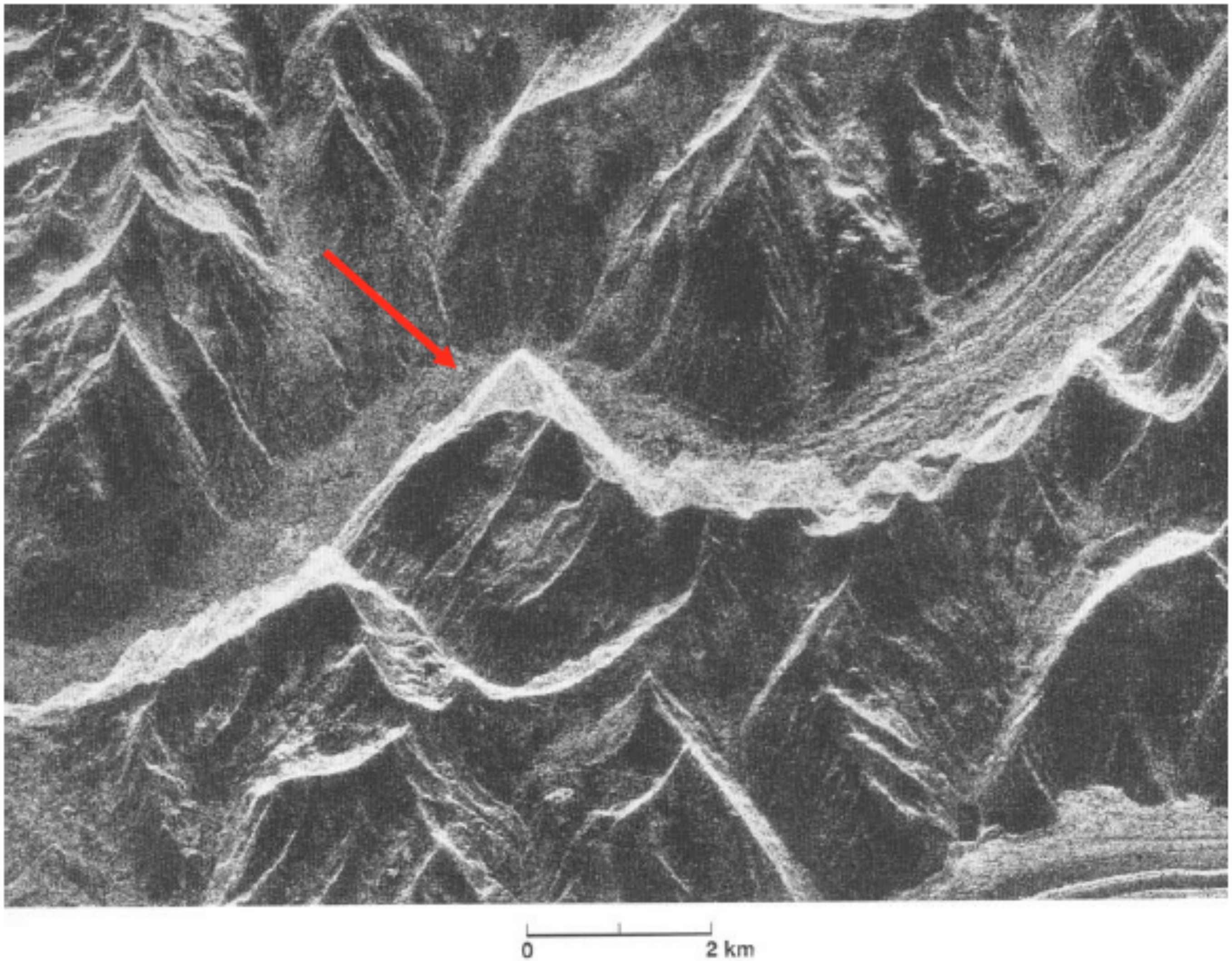

Layover Example

- Mount Fujiyama, Japan. Radar illumination from the top.

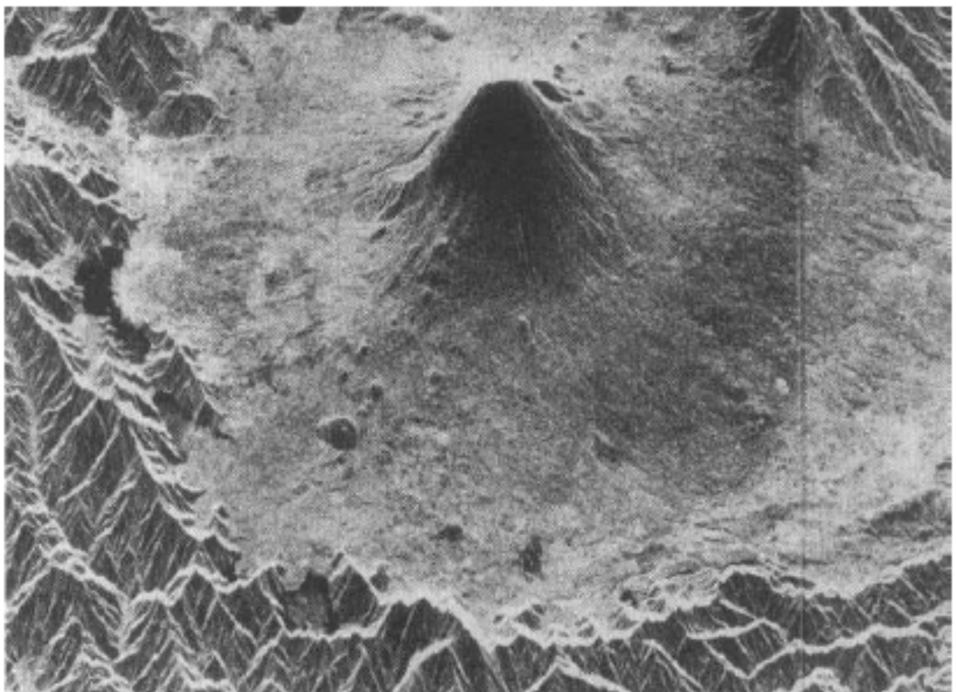

A. ERS-1 image acquired with a 67° depression angle.

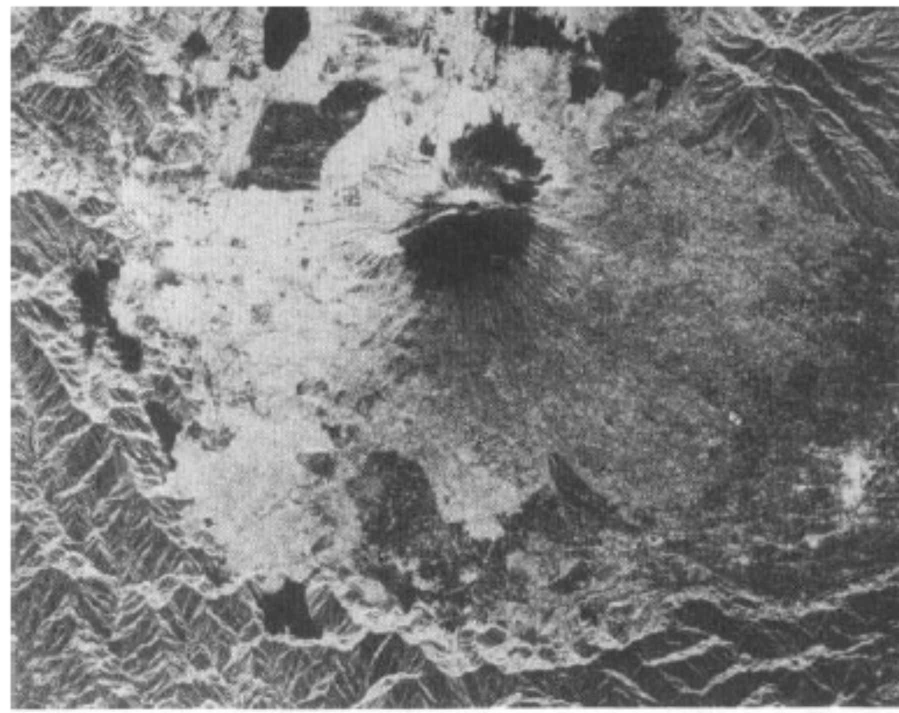

B. JERS-1 image acquired with a 55° depression angle.

Layover example - Mt. Shasta

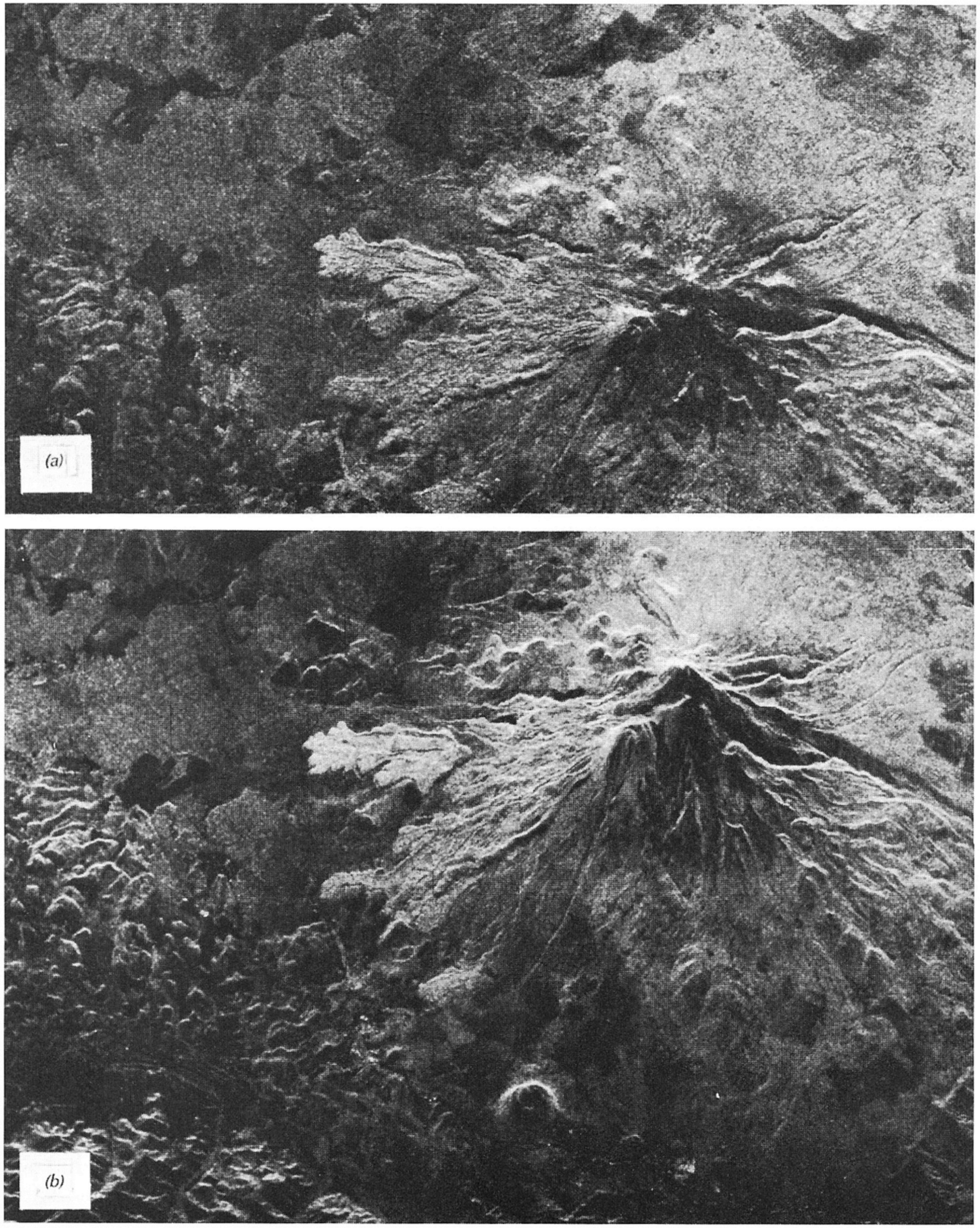

Figure 8.38 SIR-B images, Mt. Shasta, CA, L band, mid-fall (scale 1:265,000): (*a*) 60° incident angle; (*b*) 30° incident angle. Note the severe layover of the mountain top in (*b*). (Courtesy NASA/JPL/Caltech.)

Radar Remote Sensing - Layover

Gateway Arch, St. Louis, Missouri

Radar Imaging Geometry